Cardiovascular Benefits of Moderate Exercise Training in Marfan Syndrome: Insights From an Animal Model

Aleksandra Mas-Stachurska, MD, MSc;* Anna-Maria Siegert, MSc;* Monserrat Batlle, PhD; Darya Gorbenko del Blanco, PhD; Thayna Meirelles, PhD; Cira Rubies, PhD; Fabio Bonorino, MSc; Carla Serra-Peinado, PhD; Bart Bijnens, PhD; Julio Baudin, BSc; Marta Sitges, MD, PhD; Lluís Mont, MD, PhD; Eduard Guasch, MD, PhD[†] Gustavo Egea, PhD[†]

Background—Marfan syndrome (MF) leads to aortic root dilatation and a predisposition to aortic dissection, mitral valve prolapse, and primary and secondary cardiomyopathy. Overall, regular physical exercise is recommended for a healthy lifestyle, but dynamic sports are strongly discouraged in MF patients. Nonetheless, evidence supporting this recommendation is lacking. Therefore, we studied the role of long-term dynamic exercise of moderate intensity on the MF cardiovascular phenotype.

Methods and Results—In a transgenic mouse model of MF ($Fbn1^{C1039G/+}$), 4-month-old wild-type and MF mice were subjected to training on a treadmill for 5 months; sedentary littermates served as controls for each group. Aortic and cardiac remodeling was assessed by echocardiography and histology. The 4-month-old MF mice showed aortic root dilatation, elastic lamina rupture, and tunica media fibrosis, as well as cardiac hypertrophy, left ventricular fibrosis, and intramyocardial vessel remodeling. Over the 5-month experimental period, aortic root dilation rate was significantly greater in the sedentary MF group, compared with the wild-type group (Δmm, 0.27±0.07 versus 0.13±0.02, respectively). Exercise significantly blunted the aortic root dilation rate in MF mice compared with sedentary MF littermates (Δmm, 0.10±0.04 versus 0.27±0.07, respectively). However, these 2 groups were indistinguishable by aortic root stiffness, tunica media fibrosis, and elastic lamina ruptures. In MF mice, exercise also produced cardiac hypertrophy regression without changes in left ventricular fibrosis.

Conclusions—Our results in a transgenic mouse model of MF indicate that moderate dynamic exercise mitigates the progression of the MF cardiovascular phenotype. (*J Am Heart Assoc*. 2017;6:e006438. DOI: 10.1161/JAHA.117.006438.)

Key Words: aortic disease • endurance exercise • fibrosis • Marfan syndrome • myocardiopathy

Marfan syndrome (MF) is a connective tissue disorder caused by mutations in the gene encoding fibrilin-1 (*FBN1*), a connective tissue protein.[1] *FBN1* provides structural and elastic support to a variety of tissues by modulating the biogenesis and homeostasis of elastic fibers as well as the availability and activity of transforming growth factor-β family members.[2] Important insights on the molecular mechanisms involved in the pathogenesis of MF have been reported.[3] Major efforts have focused on uncovering the mechanisms of

aortic root dilation leading to dissection and rupture, a hallmark of MF that critically determines survival. Advances in basic research have recently been translated into clinical trials with the aim of pharmacological interference with the progression of aneurysm, predominantly testing β-blockers and angiotensin II receptor antagonists.[4] Unfortunately, most trials have failed to demonstrate improvement in the progression of aortic dilation, and prophylactic and timely surgical intervention remains the only lifesaving measure.[5]

Clinical Perspective

What Is New?

- Dynamic sports are strongly discouraged in Marfan patients on the basis of potential deleterious cardiovascular effects, but evidence supporting this recommendation is lacking.
- Our study in a murine model of Marfan syndrome suggests that moderate, endurance exercise for 5 months blunts aortic dilation and Marfan-associated cardiomyopathy.

What Are the Clinical Implications?

- If confirmed in well-designed studies in humans, the inclusion of cardiac rehabilitation programs in the therapeutic approach for patients with Marfan syndrome.
- The effects of more intense exercise or other types of sport other than endurance training still need to be studied.

Mitral valve prolapse often accompanies MF and could evolve into a secondary cardiomyopathy. However, recent reports suggest that cardiomyopathy could also be a primary manifestation of MF.[6,7] Other well-known systemic manifestations of MF include bone overgrowth, pulmonary emphysema, and evident myopathy, the latter being a consequence of the inability to repair muscle tissue injury and to increase skeletal muscle mass despite physical exercise.[8]

Regular physical activity is an efficient therapeutic approach to reduce the burden of cardiovascular diseases in the general population. Among other benefits, it improves left ventricular (LV) function and tissue perfusion, lowers blood pressure (BP), and reduces chronic low-grade inflammation.[9] To meet the higher metabolic demands that exercise entails, the cardiovascular system develops remarkable structural and functional changes in a remodeling process termed athlete's heart, whose features are markedly influenced by which sport is practiced. Exercise can be categorized as static (eg, weightlifting) and dynamic (eg, distance running), with very different physiological responses to each type of exercise. Although most sports include a mixture of both components, static exercise is characterized by increased BP and concentric LV hypertrophy, while volume overload and eccentric LV hypertrophy is typical in dynamic exercise.[10] Importantly, the exercise-induced remodeling process also affects the ascending aorta. In this respect, regular physical activity prompts a mild but significant aortic root dilatation, which is greater for practitioners of more dynamic sports, compared with static sports.[11]

Since dynamic physical training promotes cardiovascular extracellular matrix remodeling, changes in the aforementioned exercise-induced cardiovascular parameters will have a special impact on patients with inherited diseases, such as MF, that lead to abnormal extracellular matrix remodeling.

Consequently, it is assumed that exercise-induced extracellular matrix remodeling is adverse in these patients and worsens the progression of the aortic dilatation and cardiomyopathy. On the basis of this reasoning, dynamic physical activity has been strongly discouraged in MF patients.[12] However, no evidence is available to support this recommendation.[13]

Our aim was to evaluate the impact of dynamic exercise on the ascending aortic dilation and the cardiomyopathy in MF. We implemented a modest-to-moderate endurance exercise model, as this is the level of exercise most widely practiced by the general population. The experimental working model we selected was a heterozygous mouse line carrying a targeted mutation (C1039G) in exon 25 of the *Fbn1* gene,[14] representative of the most common class of mutations causing human MF. This murine model captures many of the clinical manifestations of MF, including aortic dilatation, cardiomyopathy, lung abnormalities, and skeletal deformations and myopathy.

Methods

Animals and Experimental Design

Fbn1$^{C1039G/+}$ mice were obtained from Jackson Laboratory (Bar Harbor, ME 04609, EE UU) and used as a validated MFS animal model. Both Wild Type (WT) and *Fbn1*$^{C1039G/+}$ mice (hereinafter, Marfan [MF] mice) were bred on a C57BL/6 background. Comparisons were made between contemporary littermates. All mice were housed in a controlled environment (12/12-hour light/dark cycle) and provided with ad libitum access to food and water. All animals were weighed once a week throughout the duration of the experiment. Animal care and experimentation conformed to the European Union (Directive 2010/63/UE) and Spanish guidelines (RD 53/2013) for the use of experimental animals. Ethical approval was obtained from the local animal ethical committee (Comitè Ètic d'Experimentació Animal CEEA).

Training Protocol

A group of WT and MF mice were randomly conditioned to run in a treadmill (Ex groups). After a 2-week adaptation period in which treadmill speed and slope and training duration were progressively increased, stable regimens were reached. Eventually, Ex mice ran at 20 cm/s, with a 12° positive slope for 60 minutes/d, 5 days/wk (Monday–Friday) for 5 months (from the age of 4 to 9 months). Training was performed in the afternoon, as close as possible to the dark (active) cycle to allow animals to rest during the light phase before training. A metallic grid at the back of the treadmill delivered a constant intensity (≈2 mA) electric shock upon

contact and motivated mice to keep running. In this training protocol, electric shocks were virtually absent in all animals. All training sessions were monitored by an experienced investigator to ensure proper running and lack of stress. Parallel WT and MF groups not undergoing training served as sedentary (Sed) controls. Sample size at the beginning of the experimental protocol was WT-Sed n=11 (5 male, 6 female); MF-Sed n=9 (5 male, 4 female); WT-Ex n=10 (5 male, 5 female); MF-Ex n=10 (5 male, 5 female).

Blood Pressure Assessment

Systemic blood pressure was noninvasively measured in all mice by a tail cuff system (Panlab NIPB system, consisting of control unit LE5007 and the automatic heater and scanner for 6 mice, LE56506). Briefly, mice were placed in a warming restrainer (34°C), with the tail carefully inserted into an inflatable cuff. Systolic blood pressure (SBP) and diastolic blood pressure (DBP) were automatically measured. Mean BP was calculated as $1/3 \times SBP + 2/3 \times DBP$.

Before initiating the exercise protocol, all mice were placed in the setup as many times as needed until they became adapted, thereby minimizing stress associated with the procedure. BP was thereafter measured at baseline, and after 1, 2, 3, and 5 months of training.

Echocardiography

Two-dimensional transthoracic echocardiography was performed in all animals, with 1.5% inhaled isoflurane administered to the animals. Each animal was scanned twice: at baseline and at the end of the experiment, at least 24 hours after the final exercise session. Images were obtained with a 10 to 13-MHz phased-array linear transducer (IL12i GE Healthcare, Madrid, Spain) in a Vivid Q system (GE Healthcare, Madrid, Spain). Images were all recorded and later analyzed offline using commercially available software (EchoPac v. 108.1.6, GE Healthcare, Madrid, Spain).

The aortic root and ascending thoracic aorta were measured in a parasternal long-axis view. Both the maximum and minimum diameters (inner edge to inner edge) were measured at the aortic sinus level (for the aortic root) and at 1 mm above the sinotubular junction (for the ascending aorta). The aortic root dilation rate was calculated as the diastolic aortic root diameter at the 9-month time-point minus the diastolic aortic root diameter at the 4-month time-point.

The M-mode spectrum was traced at the papillary muscle level in a parasternal short axis view, where LV dimensions at both end-diastole (LVDD) and end-systole (LVSD) were measured. The anterior wall and posterior wall thickness at end-cardiac diastole were also measured. LV ejection fraction (LVEF) was subsequently calculated as follows:

$$LVEF = \frac{LVDD^3 - LVSD^3}{LVDD^3} \times 100$$

The presence of postsystolic shortening (PSS) was assessed in M-mode recordings obtained with the cursor positioned in the LV basal septum in a parasternal long-axis view. An animal was considered to have PSS if a "double peak sign" was consistently identified. The "double peak sign" consists of a normal-shaped deformation pattern (first peak) during the ejection period followed by an ongoing deformation (second peak) after aortic valve closure.

Aortic Pulsatility and Aortic Stiffness Estimation

Aortic pulsatility was used as a distensibility estimator, and calculated as follows:

$$Pulsatility = \frac{Ao_{max} - Ao_{min}}{Ao_{min}} \times 100$$

where Ao_{max} stands for maximum aortic diameter, and Ao_{min} stands for minimum aortic diameter. The final result is shown as percentage (%).

Aortic stiffness was calculated using the BP and echocardiographic aorta diameter in vivo. For each animal, the following formula was used to calculate the β-index:

$$\beta = \frac{\log\left(\frac{SBP}{DBP}\right)}{\left(\frac{Ao_{max} - Ao_{min}}{Ao_{min}}\right)}$$

where SBP stands for systolic blood pressure, DBP stands for diastolic blood pressure, Ao_{max} stands for maximum aortic diameter, and Ao_{min} stands for minimum aortic diameter. The final result is dimensionless.

Euthanasia and Sample Collection

Nine-month-old mice were euthanized with an overdose of isoflurane inhalation and ascending aorta, heart samples and the vastus medialis muscle were quickly excised, immersed in cold physiological serum, and processed as described below.

Aortic Collagen Deposition and Elastic Fiber Ruptures

The thoracic aorta was cut just above the aortic valve, and the ascending aorta was subsequently fixed in formaldehyde and embedded in paraffin. Four-micron-thick sections were obtained and stained with Verhoeff-Van Gieson stain. Sections were examined using a Leica DMRB microscope (×40). Two blinded investigators quantified aortic elastic fiber ruptures by fiber discontinuities per longitude in at least 4

representative images in each animal, and the average was calculated for each animal.

Furthermore, sections were stained with picrosirius red to analyze collagen deposition. Six representative images were taken of each animal using the brightfield and polarized light of a Leica DMRB microscope. The tunica media was delimited using the brightfield images and corresponding polarized light images were used to quantify picrosirius red–stained collagen deposition.

Left Ventricle Histological Study

The whole heart was fixed in formaldehyde and transversally cut through midventricle in 2 blocks (basal and apical blocks). Both blocks were embedded in paraffin wax and 4-μm-thick sections were obtained from the basal block and layered in poly-L-lysine–coated glass slides. The slides were stained with picrosirius red. Intramyocardial collagen deposit was quantified, excluding the endomyocardial, epicardial, and perivascular fibrosis. Pictures (×40) of 3 different representative areas of left ventricle (LV) were taken from each sample and the mean percentage of collagen deposition was calculated.

In order to assess intramyocardial vessel remodeling, pictures of both right ventricle and LV were taken (×100) whenever a vessel was identified. Approximately 10 intramyocardial arteries were localized and different measurements were taken: perivascular area (A), limited by perivascular fibrosis; external area (Ae), limited by outer tunica adventitia; and internal area (Ai), limited by internal elastic lamina (Figure S1). The area of the lumen, tunica media, and perivascular fibrosis were all normalized to the vessel size (Ae) to exclude any bias in selecting vessels. All pictures were taken with an Olympus BX41TF microscope and DP73 camera. Blinded quantification of vascular remodeling and collagen deposition was performed with ImageJ 1.48v.

Skeletal Muscle Histochemistry

At the euthanasia, the *vastus medialis* was excised by transecting the muscle origins and insertions. Muscles were placed on a mounting block and frozen in liquid nitrogen–cooled isopentane (2-methylbutane). Samples were sectioned at 5 μm at −20°C. Cross-cryosections were stained with NADH-tetrazolium reductase to examine the oxidative capacity of muscle fibers. Based on their NADH content, fibers were classified as type I (oxidative), type IIA (aerobic glycolytic), and type IIB (anaerobic glycolytic). Fiber types of the whole muscle section were counted using an Olympus BX51 microscope connected to a movable platform and the computer-assisted stereological toolbox (CAST) software count tool.

Capillaries were identified with the endothelial-specific marker CD31. Briefly, muscle sections were incubated with

rat anti-CD31 monoclonal antibody, clone MEC 13.3 (BD Biosciences) and a donkey anti-rat IgG secondary antibody (Jackson Immunoresearch). CD31-positive structures of muscle cryosections were counted using an Olympus BX51 microscope connected to a movable platform and the computer-assisted stereological toolbox (CAST) software count tool.

Exploration of Sex Differences

After conducting main analyses, the effect of sex was explored in further statistical analyses. The effect of sex was explored in BP, histological analyses (aortic fibrosis and elastic fiber ruptures, LV fibrosis, intramyocardial arteries assessment), and in most echocardiographic variables (aortic root diameter, LVSD, LVDD, anterior wall, posterior wall, and LVEF). The effect of sex in PSS was not studied because the low sample size in each of the groups made analyses of a categorical variable meaningless. Because sex is known to heavily influence body weight, only de-aggregated data are shown.

Statistical Analysis

All results for continuous variables are reported as mean ±SEM. Because no mice had yet been trained, only the effect of genotype (ie, WT versus MF) was analyzed at the 4-month time-point; a nonpaired *t* test was used for comparisons in these cases. When 2 main factors were present in the study design (eg, genotype×training), data were modeled in a 2-way ANOVA that included the 2 main factors and their interaction. Data with a repeated measurement factor (eg, several measurements over time) were analyzed with a linear mixed-effects model. For intramyocardial vascular remodeling, each analyzed vessel was nested within mouse and a random effect was included in the model. When a significant interaction was found, least significant differences (LSD)-adjusted pairwise comparisons are reported. In the absence of a significant interaction, significant main effects, if present, are reported. A normal distribution of the residuals (Q-Q plot and Shapiro–Wilks) was checked for all analyses.

Categorical variables (eg, PSS presence) are reported as percentages. The proportion of mice with PSS in all groups at baseline was compared with a Fisher exact test. Change of PSS over time (from 4- to 9-month time-points) in MF was assessed through a McNemar test.

Mouse survival is shown on a survival curve and comparisons carried out with a log-rank test.

After main analyses were conducted, the effect of sex was tested for all analyzed parameters by adding the Sex factor and all their interactions. In the case that the Sex factor or any of its interactions was significant, this is reported.

A $P \leq 0.05$ was considered significant. Statistical analysis was carried out with Stata v13 (College Station, TX, USA) and Graphpad Prism v6.0 (GraphPad Software, Inc, USA).

All echocardiogram and histological measurements were carried out in a blinded manner of genotype and treatment group.

Results

All mice subjected to exercise adequately adapted to the training protocol. Two MF mice allocated to the Sed group (1 male and 1 female mouse) died early in the experimental protocol; no other deaths occurred in any other group (Figure S2). Necropsy was not performed and the cause of death remained unknown for both dead animals. The difference in mortality between groups did not reach significance ($P=0.063$).

We next tested whether the intensity of physical activity promoted peripheral muscle adaptation. In *vastus medialis,* we found a switch in the oxidative status of muscular fibers in trained WT mice in comparison to sedentary WT mice. However, capillary density evidenced by CD31-positive endothelial cells staining did not differ among groups, most likely because of the large variability observed in the trained group (Figure S3).

Because sex critically determines weight, results are shown after sex-stratification. Over the 5-month training period, weight gain was similar in all groups, both for male and female mice (Figure 1A). There were no differences in BP measurements at baseline between WT and MF mice (SBP was 130 ± 2 versus 134 ± 3; DBP was 79 ± 2 versus 79 ± 2; WT versus MF). In Sed animals, BP remained similar throughout the experimental period. In contrast, MF-Ex mice developed a higher SBP compared with WT-Ex, with no changes in DBP or mean BP (Figure 1B). However, there were no significant differences between trained WT and MF mice and their Sed littermates, likely because the statistical power was too low to uncover whether these differences arose from a decreased BP
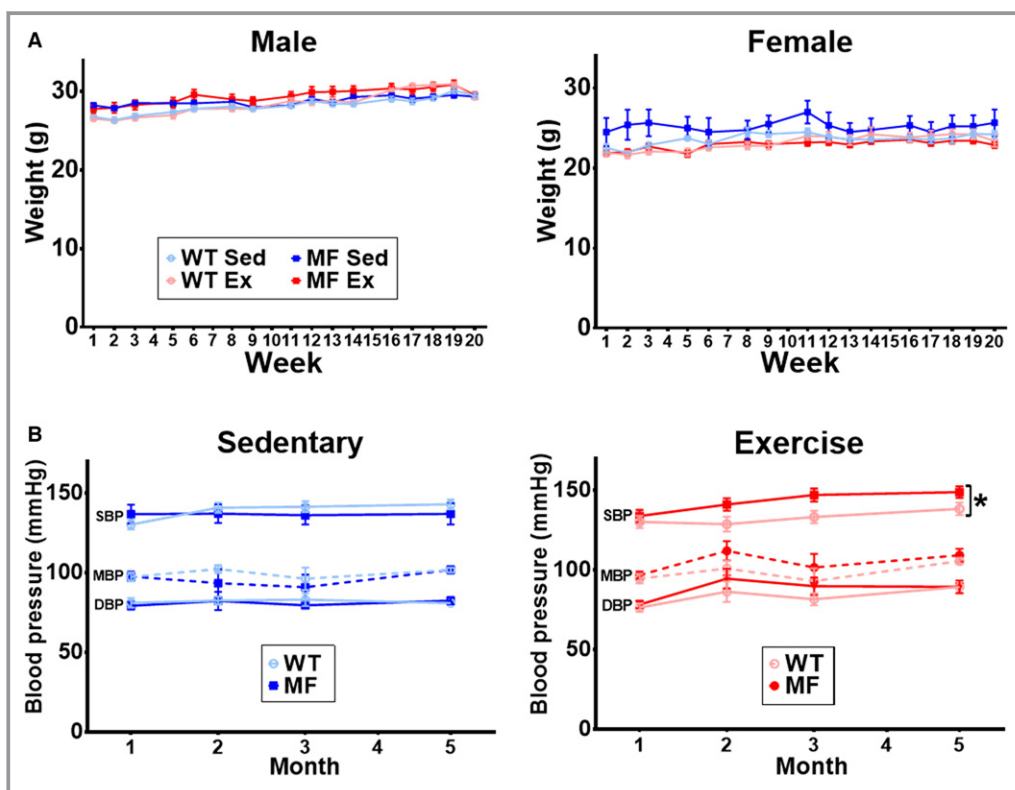

Figure 1. Weight and blood pressure measurements in sedentary and trained WT and MF mice. A, Weight measurement during the experimental protocol (weeks 1–14) in all animals; results are shown separately for male and female mice (beginning the experiment, for male animals: n=5 for WT-Sed, MF-Sed, MF-Sed and MF-Ex; for female animals: n= 6 for WT-Sed; n=4 for MF-Sed; n=5 for WT-Ex; n=5 for MF-Ex). Analysis was performed with mixed-effects models; no significant differences were found between groups. B, Blood pressure was measured in all groups at 1, 2, 4, and 5 mo (beginning the experiment: n=11 for WT-Sed, n=9 for MF-Sed, n=10 for WT-Ex, n=10 for MF-Ex). Analysis was performed with mixed-effects models. No differences were found in Sed animals. In trained mice, a significant genotype effect was observed ($P<0.05$). *$P<0.05$. Ex indicates trained group; MF, Marfan; Sed, sedentary group; WT, wild-type.
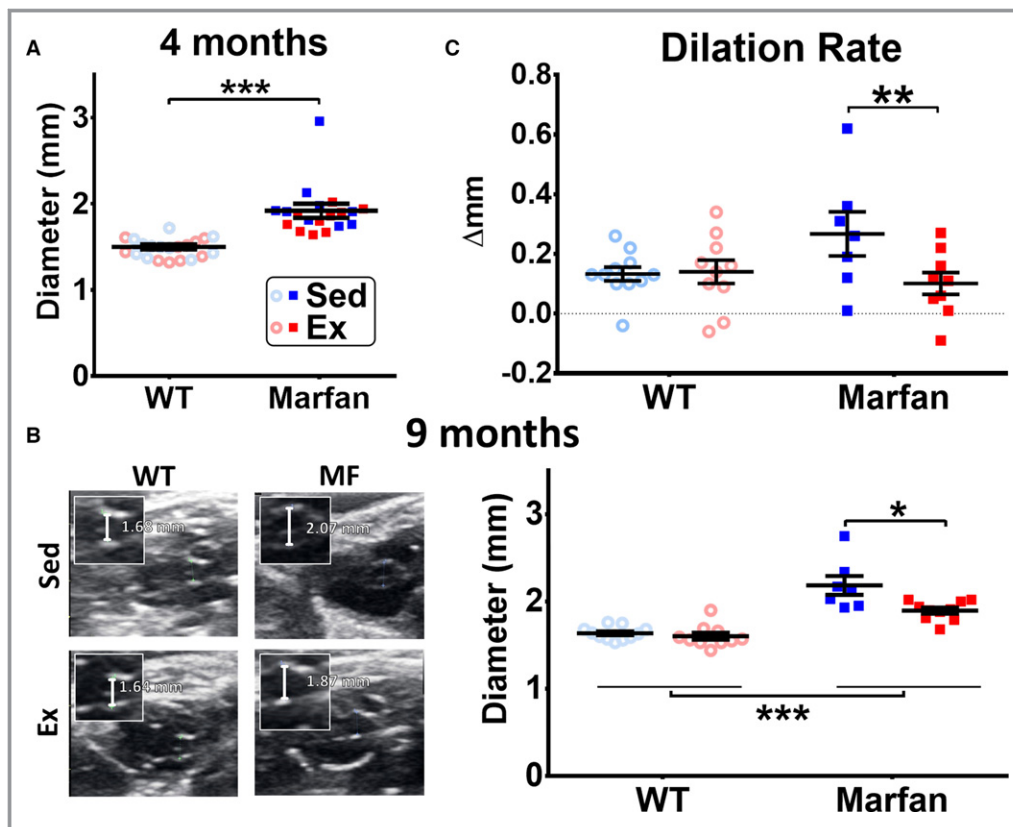
Figure 2. Echocardiographic measurements in sedentary and trained WT and MF mice. A, Average aortic root size at the 4-mo time-point in WT and MF mice (n=21 for WT, n=19 for MF). Analysis used a nonpaired *t* test. B, Aortic root size after the experimental protocol (9 mo) in all groups (n=11 for WT-Sed, n=7 for MF-Sed, n=10 for WT-Ex, n=10 for MF-Ex). Representative echocardiographic images of the aortic root size in all groups (left panel). Quantitative analysis (right panel) was done with 2-way ANOVA. A significant (genotype×training group) interaction was found (*P*<0.05); pairwise comparisons (training group within genotype and genotype within training group) are shown. C, Dilation rate in all groups (n=11 for WT-Sed, n=7 for MF-Sed, n=10 for WT-Ex, n=9 for MF-Ex). In 2-way ANOVA, genotype×training group interaction was found (*P*<0.05); pairwise comparisons (Sed vs Ex within each genotype) are reported: **P<0.05; **P<0.01; ***P<0.001. Ex indicates trained group; MF, Marfan; Sed, sedentary group; WT, wild-type. Open circles represent WT mice, closed squares represent Marfan mice; blue symbols are sedentary mice, red symbols are trained mice.

in trained WT mice, an increased BP in trained Marfan mice, or a combination of both. Although BP was lower in female- than in male-trained mice, sex had no impact on the effect of exercise (Figure S4).

Moderate Exercise Slows the Progression of Aortic Root Dilation in Marfan Mice

All groups were subjected to echocardiographic evaluation of the aortic root (Figure 2). In accordance with clinical data and previous reports, 4-month-old MF mice had an enlarged aortic root at the beginning of the study (Figure 2A). All groups were scanned again at the end of the experimental period (9 months), with representative echocardiographic images shown in Figure 2B. In WT mice, moderate exercise did not induce changes in the size of the aortic root. In MF mice

subjected to exercise, however, aortic root diameter was smaller than in their Sed littermates (Figure 2B). To more accurately assess changes in aorta diameter over time, aortic root dilation rate was defined as the change in the aortic root size over the 5-month experimental protocol and was calculated from mouse-by-mouse aortic root size (Figure S5). Dilation rate in MF-Sed mice was twice that of WT (Δmm, 0.27±0.07 versus 0.13±0.02, respectively; Figure 2C). Remarkably, this parameter was blunted in trained MF mice, becoming comparable to the WT dilation rate (MF-Ex Δmm 0.10±0.04; Figure 2C). Aorta measurements at a more distal level yielded similar results: the ascending aorta was dilated at baseline in MF mice and dilation was blunted in trained mice (Figure S6).

The aortic root in MF patients is stiffer than in healthy individuals.[15] In our mice, aorta mechanical properties were
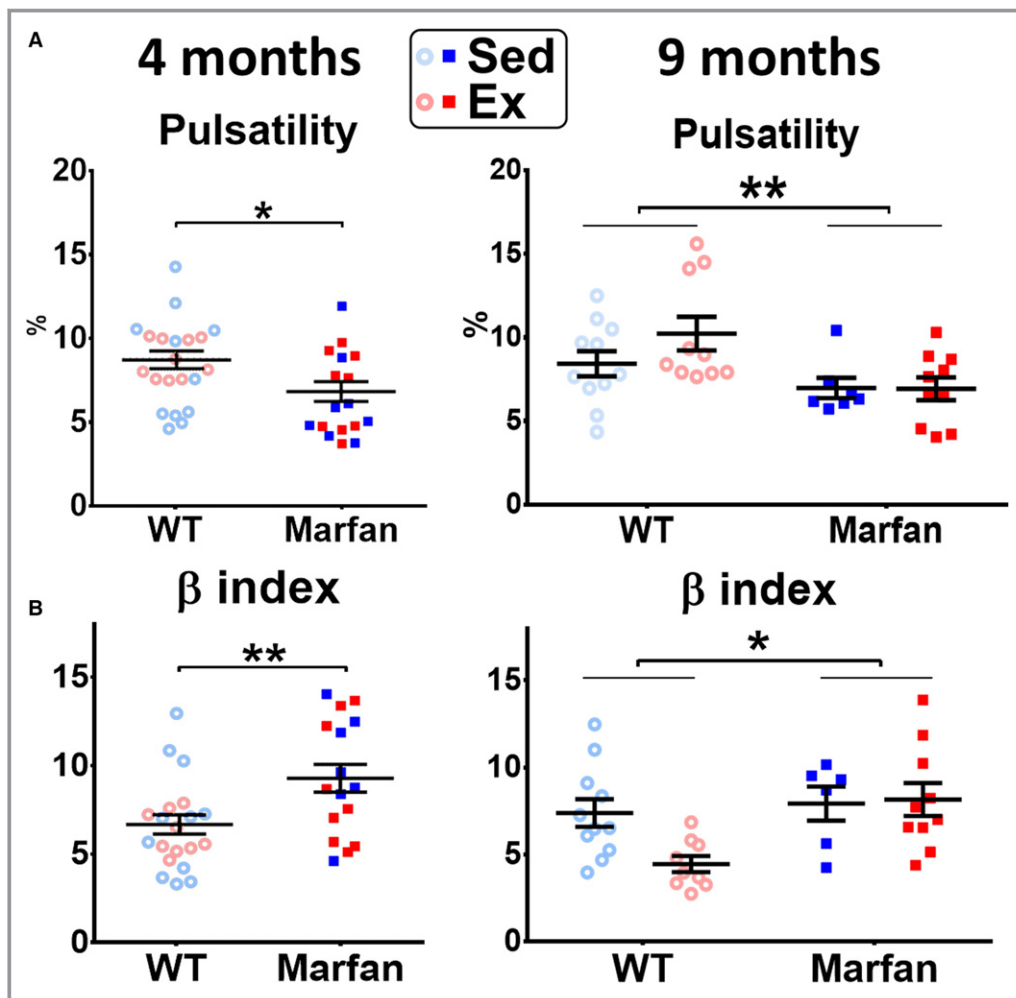
Figure 3. Aortic root pulsatility and stiffness in sedentary and trained WT and MF mice. Aortic root pulsatility (A) and β-index (B) at baseline (n=21 for WT, n=17 for MF; 4-mo-old mice; nonpaired *t* test) and at the end of the experimental training (n=11 for WT-Sed, n=7 for MF-Sed, n=10 for WT-Ex, n=10 for MF-Ex; 9-mo-old mice; 3-way ANOVA test). *$P<0.05$; **$P<0.01$. Ex indicates trained group; MF, Marfan; Sed, sedentary group; WT, wild-type. Open circles represent WT mice, closed squares represent Marfan mice; blue symbols are sedentary mice, red symbols are trained mice.

estimated by combining in vivo data obtained from BP measurements and echocardiographic maximum and minimum aorta diameters. At 4 months, we observed significant differences in the aortic root expansibility (pulsatility) between WT and MF mice, which is indicative of a loss of elasticity (Figure 3A, left panel). At 9 months, differences between WT and MF persisted. WT-Ex mice showed a slight increase in pulsatility compared with WT-Sed, but it did not reach statistical significance. MF-Ex mice showed indistinguishable pulsatility from MF-Sed (Figure 3A). Subsequent calculation of the β-index at baseline (4 months) supported increased aortic root stiffness in MF mice compared with WT mice (Figure 3B). After the exercise training, β-index (aortic stiffness) significantly improved in WT but not in MF mice.

Aortic Structural Abnormalities Remain Unaltered in Trained Marfan Mice

The most representative histological damage evaluated in MF mice is the rupture of elastic fibers in the tunica media of the ascending aorta. As expected, we observed a significant increase in the number of elastic lamina ruptures in MF mice, compared with WT animals (Figure 4A, upper panels and 4B for quantitative analysis). Remarkably, exercise did not increase lamina ruptures, indicating no additional structural damage in the tunica media of MF aorta.

Next, we examined the collagen content as a compensatory mechanism to the elastic fiber ruptures. In Sed mice, the tunica media had more collagen staining in MF than in WT animals (Figure 4A, middle and lower panels). As with elastic fibers,
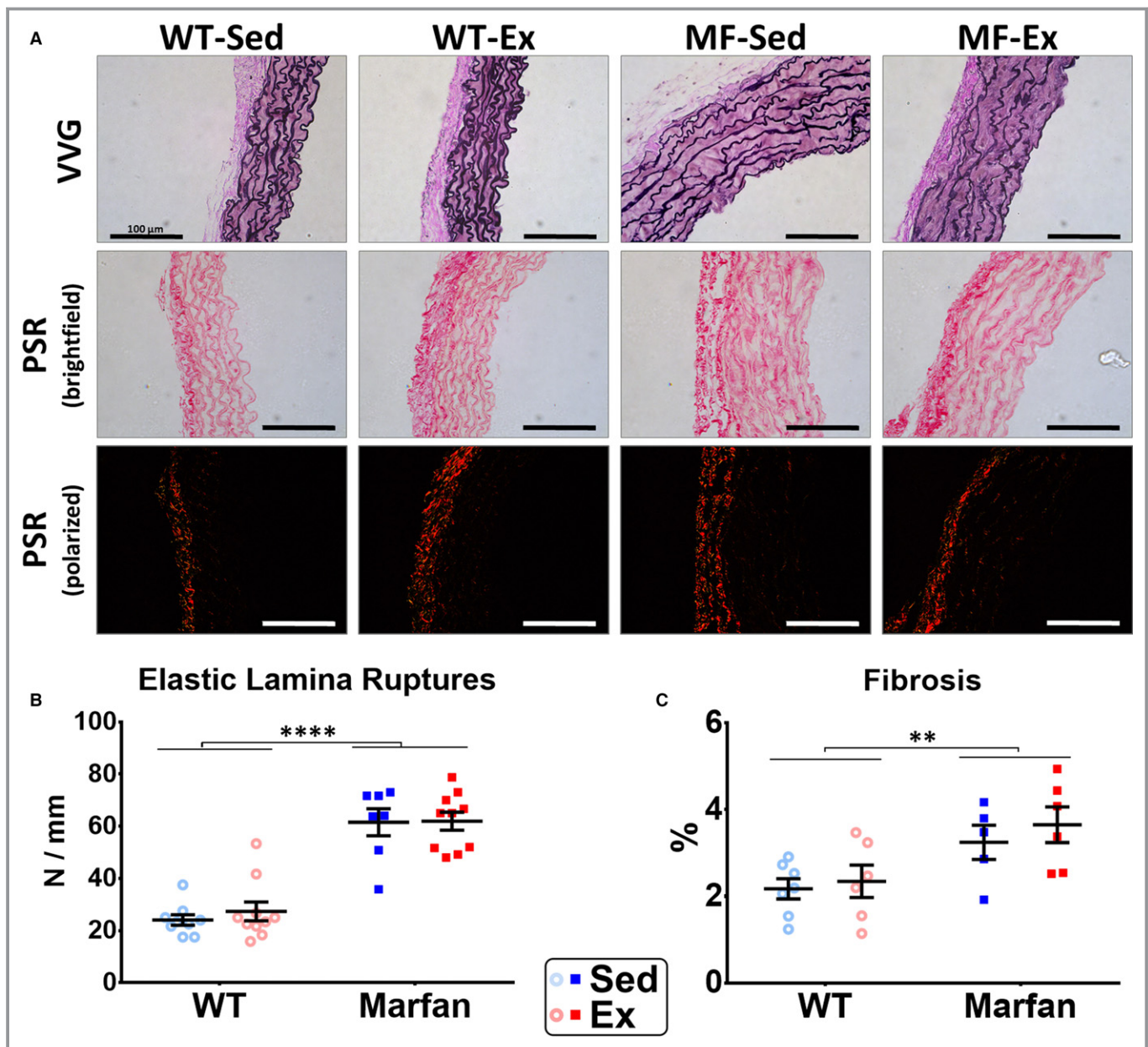
Figure 4. Aorta histological analyses in sedentary and trained WT and MF mice. A, Representative images of elastic laminae (stained in black by Verhoeff-Van Gieson [VVG] staining, upper panel) and collagen content (stained by picrosirius red [PSR]), visualized under brightfield or polarized light in the middle and lower panels, respectively. B, Quantitative analysis of elastic laminae ruptures (n=9 for WT-Sed, n=7 for MF-Sed, n=10 for WT-Ex, n=10 for MF-Ex). Two-way ANOVA showed no interaction but a genotype (WT vs MF) effect was evident (****P<0.0001). C, Quantitative analysis of fibrosis (n=7 for WT-Sed, n=5 for MF-Sed, n=6 for WT-Ex, n=6 for MF-Ex). Two-way ANOVA showed no interaction but a genotype effect was clear (**P<0.01). Bars = 100 μm. Ex indicates trained group; MF, Marfan; Sed, sedentary group; WT, wild-type. Open circles represent WT mice, closed squares represent Marfan mice; blue symbols are sedentary mice, red symbols are trained mice.

dynamic exercise did not have any impact on these differences between WT and MF mice (Figure 4C, quantitative results).

Exercise Improves Marfan-Associated Cardiac Hypertrophy

The potential impact of moderate exercise on the heart was also examined, with LV dilation and hypertrophy observed at baseline in MF mice (Table 1). After the 5-month training protocol, LV hypertrophy evaluated by echocardiography significantly regressed in MF-Ex mice, as shown by decreased anterior wall and posterior wall diameters (Table 2). A nonsignificant decrease in LVDD and LVSD was also observed.

PSS is attributed to differential loading or contractility in neighboring segments and, when perfusion is normal,

Table 1. Echocardiographic Measurements of LV Structural and Functional Parameters in All Groups at 4 Months (Before Training)

	Wild Type (n=21)	Marfan (n=17)
AW, mm*	0.59±0.02	0.65±0.01
LVEDD, mm*	3.75±0.08	3.98±0.07
PW, mm*	0.57±0.02	0.63±0.02
LVESD, mm	2.54±0.08	2.76±0.06
LVEF, %	69±2	67±1

AW indicates anterior wall; LV, left ventricle; LVEDD, left ventricle end-diastolic diameter; LVEF, left ventricular ejection fraction; LVESD, left ventricle end-systolic diameter; PW, posterior wall.
*$P<0.05$, wild-type vs Marfan.

predominantly reflects pressure overload. More specifically, it occurs when there is an imbalance between local (pressure-induced) wall-stress, contractility, and tissue structural properties.[16] PSS was more common in MF than in WT mice at 4 months (14/17 [82%] versus 7/21 [33%], respectively; $P≤0.01$). While the presence of PSS remained unaltered (71%) at the 9-month time-point in MF-Sed mice, it showed a decreasing trend in MF-Ex mice (PSS 40%, $P=0.12$, McNemar test) (Figure 5).

As with aortae, LV changes were histologically assessed from collagen content. An evident increase in collagen deposition was observed in 9-month-old MF-Sed mice. Moderate training did not modify LV fibrosis in either the WT-Ex or MF-Ex groups (Figure 6A).

In the heart, vascular remodeling was also studied in small arteries in the LV (Figure 6B). A prominent vascular remodeling in MF mice included a narrow lumen as well as thickening and increased perivascular fibrosis (Figure 6B). Again, moderate regular exercise showed no effect.

Table 2. Echocardiographic Measurements of LV Structural and Functional Parameters in All Groups at the 9-Month Time Point

	Wild Type		Marfan	
	Sedentary	Trained	Sedentary	Trained
LVEDD, mm†	3.89±0.1	3.79±0.04	4.24±0.19	4.04±0.08
LVESD, mm*	2.65±0.06	2.61±0.07	2.95±0.18	2.73±0.1
AW, mm†	0.66±0.02	0.64±0.01	0.72±0.02	0.69±0.02‡
PW, mm*	0.65±0.02	0.63±0.01	0.73±0.03	0.68±0.02‡
LVEF, %	67±1	67±2	66±3	69±3

AW indicates anterior wall; LVEDD, left ventricle end-diastolic diameter; LV, left ventricular; LVEF, left ventricular ejection fraction; LVESD, left ventricle end-systolic diameter; PW, posterior wall; WT, wild-type.
*$P<0.05$, †$P<0.01$ WT vs Marfan.
‡$P<0.05$ vs genotype-matched sedentary group.

Effects of Exercise on Marfan-Associated Cardiovascular Remodeling Are Independent of Sex

We explored potential sex-related impacts of MF- or exercise-promoted cardiovascular remodeling. The most representative findings are shown in Figures S7 through S9. At baseline (4 months), echocardiography experiments showed that aortic dilatation and LV hypertrophy were similar in male and female MF mice (Figure S7). At the end of the experimental protocol (9 months), the protective effect of moderate exercise on aortic dilation and LV hypertrophy, both examined by echocardiography, were similar in male and female mice (Figure S8). Exploratory analyses in histology experiments suggested that LV fibrosis was reduced in trained female, but not male mice in comparison to their Sed littermates (Figure S9).

Discussion

We evaluated the effects of exercise in the MF phenotype, particularly focusing on cardiovascular remodeling. In a murine MF model, moderate exercise (1) mitigated aortic dilation, (2) did not increase aortic elastic fiber ruptures and collagen deposition, and (3) partially reversed MF-associated cardiac hypertrophy. Overall, our results suggest positive effects of moderate exercise in cardiovascular manifestations of MF.

Exercise and the Aortic Root in MF

Aortic root dilation is a hallmark of the cardiovascular phenotype of MF and a main determinant of premature mortality and morbidity. The degree of aortic dilation closely correlates with the risk of aortic dissection.[17] Factors such as an increased central pulse pressure,[18] obstructive sleep apnea,[19] or genetic predisposition based on polymorphisms in genes other than *FBN1*[20] have been proposed to influence aortic dilation rate in MF. A repetitive, pulsatile increase in aortic stretch during each exercise bout has been claimed to trigger accelerated aortic dilation.[11,12]

Contrary to this hypothesis, we showed that regular, moderate exercise does not accelerate aortic dilation rate, but rather normalizes its progression to values comparable to WT animals. Note that the aortic root was only assessed at baseline and at the end of the experimental protocol. Echocardiographic improvement was not accompanied by a restoration of the histological integrity of elastic fibers. Whereas histological and echocardiographic measurements usually present with parallel improvements, we found a clear blunt in aortic dilation in the absence of overt changes in elastic lamina fractures. It is possible that modest
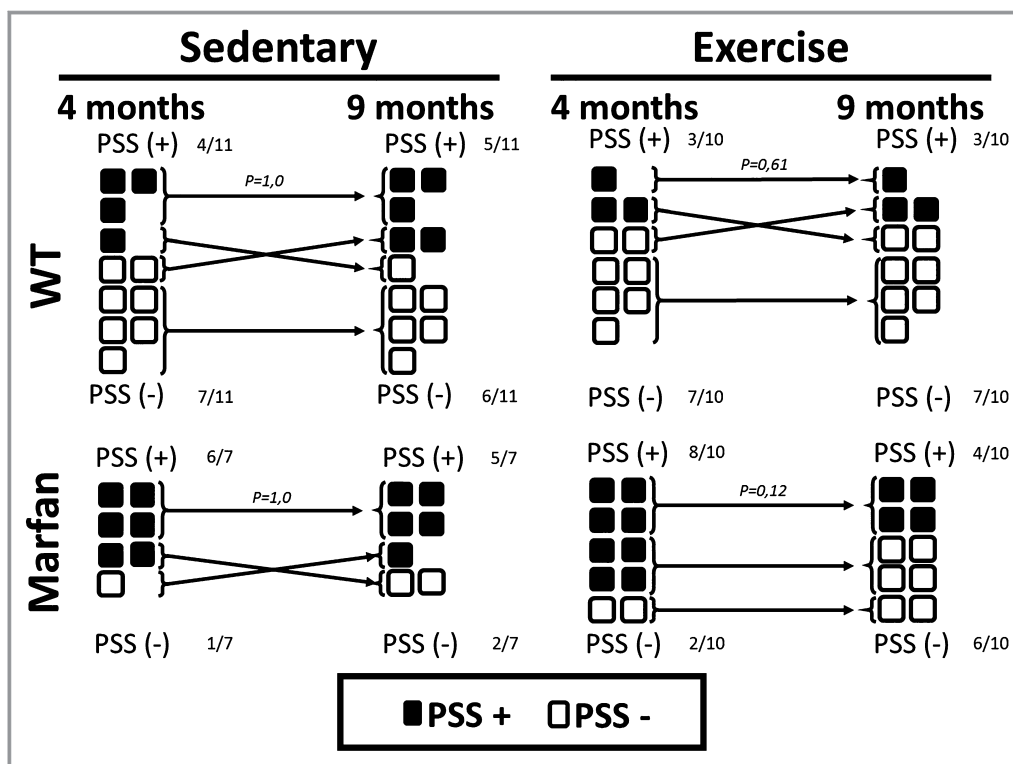
Figure 5. Cardiac hemodynamic overload (postsystolic shortening [PSS]) in sedentary and trained WT and MF mice. Number of mice with and without PSS for all groups and all time-points. Analysis done with McNemar test. MF indicates Marfan; WT, wild-type.

improvements such as the one in our work may present with nonevident histological changes. In fact, we cannot rule out the possibility that improvements in microstructural ruptures in MF-Ex mice could precede evident elastic fiber repair evaluated by regular histological approaches. Such microstructural improvements in elastic fibers might have a positive physiological impact, which can be resolved by echocardiography. Indeed, elastic abnormalities might be present in advance of evident aortic dilation,[21,22] and alterations in elastic fiber integrity are present in the nondilated portion of the thoracic aorta,[23] thereby suggesting a mismatch between aorta size and elastic properties. Moreover, other factors such as fibronectin synthesis,[24] or endothelial[25] and smooth muscle cell dysfunction,[26] may also significantly contribute to progressive aortic dilation.

The subjacent mechanism(s) behind the reduction of aortic size in exercised Marfan mice is unknown. Of note, a recent work has suggested that inducible nitric oxide synthase (iNOS) upregulation is involved in Marfan aortic dilation.[27] Interestingly, exercise has been shown to reduce iNOS expression in settings in which iNOS is heavily induced (eg, in obesity[28] and diabetes mellitus[29]). On the other hand, to date most therapeutic approaches for Marfan syndrome target BP, but BP was not reduced in our model. Similarly,

iNOS blockade normalized aortic size in MF mice while increasing BP.[27] Altogether, these results point to iNOS downregulation as an attractive potential mediator of exercise-associated benefits in MF.

Exercise and Marfan-Associated Cardiomyopathy

The most frequent and well-known cardiac manifestation of MF is mitral valve prolapse.[5] If severe, mitral prolapse and regurgitation may evolve as progressive LV dilation and dysfunction and, eventually, heart failure. Nevertheless, recent data support the existence of a primary myocardial affectation in MF patients even in the presence of competent valves.[6,7,30] Structural abnormalities in the MF cardiomyopathy include LV hypertrophy and, in some series, dilation; these may be accompanied by variable degrees of systolic dysfunction, which occasionally remains subclinical and only detectable through deformation analysis.[31] Currently, it is unclear whether this cardiomyopathy is associated with worse clinical outcomes.

Our findings in this animal model of MF concur with most of these cardiac manifestations. We show increased collagen deposition in the LV myocardium of MF mice. A similar trend was previously reported in the same mouse strain, but failed
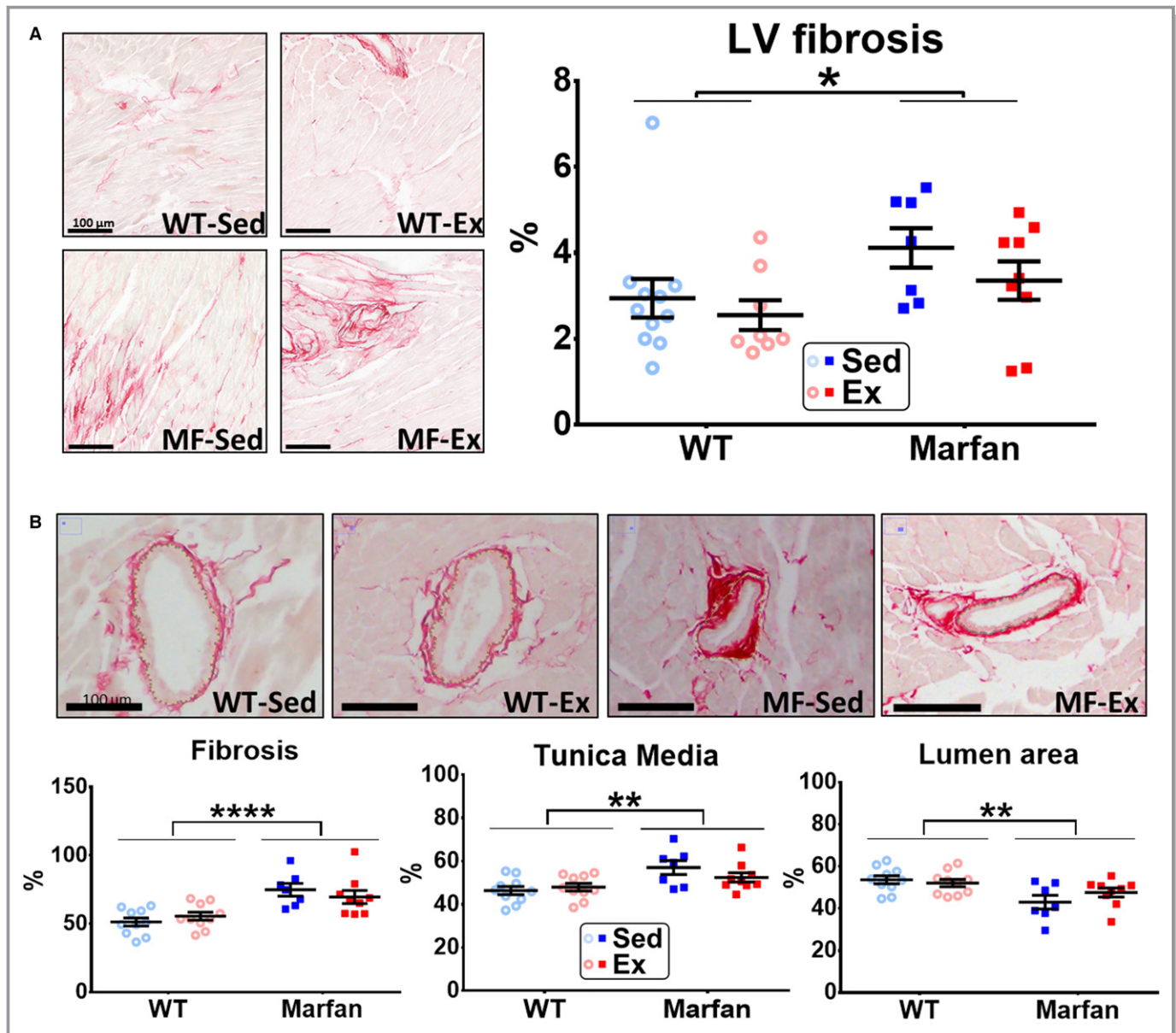
Figure 6. Histological analysis of the left ventricle in sedentary and trained WT and MF mice. A, Representative picrosirius red–stained myocardial samples of all groups (left panel) and their respective quantitative analysis (right panel); n=11 for WT-Sed, n=7 for MF-Sed, n=8 for WT-Ex, n=9 for MF-Ex. B, Histological evaluation of intramyocardial vessels (upper panel) and quantitation of the perivascular fibrosis, tunica media thickness, and lumen area (n=10 for WT-Sed, n=7 for MF-Sed, n=10 for WT-Ex, n=9 for MF-Ex). Two-way ANOVA (all measurements) showed no significant interaction, but a genotype (WT vs MF) was found for all analyses. Bars are 100 μm. *$P<0.05$; **$P<0.01$; ****$P<0.0001$. Ex indicates trained group; LV, left ventricular; MF, Marfan; Sed, sedentary group; WT, wild-type. Open circles represent WT mice, closed squares represent Marfan mice; blue symbols are sedentary mice, red symbols are trained mice.

to reach significance, likely because of the limited sample size and large intrinsic variability.[30] The clinical and physiological significance of such fibrosis is unknown, but could contribute to some characteristics of MF cardiomyopathy. It is possible that both myocardial fibrosis and hypertrophy underlie the diastolic dysfunction observed in patients with MF.[32] Moreover, fibrosis is a hallmark of cardiac arrhythmogenesis and likely contributes to the increased burden of ventricular arrhythmias in these patients.[33]

Our results indicate a positive impact of moderate exercise on MF cardiomyopathy as evidenced by an antihypertrophic effect and the absence of deleterious effects on LV myocardial fibrosis (Table 2). This is consistent with the role of physical activity in other cardiac conditions reported in human and animal models. Moderate exercise improves cardiac remodeling in hypertensive patients[34] and blunts cardiac hypertrophy and fibrosis in a hypertrophic cardiomyopathy mouse model.[35]

Clinical Implications

Whereas moderate aerobic physical activity in healthy individuals and in patients with some cardiovascular disorders is largely acknowledged,[9] MF patients are usually excluded or largely limited from obtaining these positive effects by current recommendations. Moderate-to-strenuous dynamic exercise is prohibited for these patients and only low-dynamic sports such as bowling, golf, and archery are allowed.[12] Nevertheless, this recommendation (level of evidence C) lacks clinical or experimental supporting data.[12]

Our results suggest not only that moderate physical activity may be safe, but that it might prove beneficial in MF patients by decelerating the aortic dilation rate and improving signs of cardiac hemodynamic overload. If our results were reproduced in humans, physical activity of moderate intensity should not only be allowed, but encouraged in patients with MF. This idea is supported by a case report showing that a cardiovascular physical therapy program reversed LV dilation and hypertrophy in a patient with MF.[36]

It is important to note that the present results reflect changes promoted by light or moderate endurance training. More intense forms of physical activity or other sorts of exercise may yield opposite results. Current evidence suggests that a U-shaped relationship between exercise and outcomes exists for outcomes such as atrial fibrillation, ventricular arrhythmias, or even atherosclerosis.[37] Under this hypothesis, low doses of physical activity should yield beneficial effects, but might turn deleterious at strenuous doses in healthy individuals.[38] A U-shaped relationship has also been found in inherited cardiomyopathies. Competitive exercise accelerates the progression of arrhythmogenic right ventricular cardiomyopathy,[39] although moderate exercise was shown to be safe.[40] Further research is needed to explore the potential benefits of encouraging light or moderate physical activity in patients with MF.

Limitations

First, the *Fbn1*[C1039G/+] mouse strain presents a low risk of aortic dissection and relatively long lifespan. During the 5-month experimental period, only 2 of 22 MF mice died, neither of them in the MF-Ex group. Whether our results would similarly apply to individuals at high risk remains unknown. Second, the translation of results obtained in mouse models to human beings, and interpretation of the exercise intensity in human terms, warrants caution. Reported data suggest that our study assessed moderate exercise intensity.[41] Moreover, the lack of a clear phenotype for athlete's heart, including LV hypertrophy and dilation parameters, further supports the characterization of the exercise as moderate. Third, a rigorous measurement of aortic root stiffness requires invasive blood pressure recordings. We measured the noninvasive blood pressure (tail-cuff) to estimate aortic stiffness, but it remains controversial whether this method provides a robust estimation of central BP in mice. Last, valve regurgitation, either mitral or aortic, is a frequent clinical observation in MF patients, but they were not assessed in our mice. It is therefore possible that they could modify the effect of exercise in the cardiovascular phenotype of MF. Nevertheless, we could not envisage any clustered response to exercise for aortic dilation, fibrosis, or any of the echocardiographic parameters, thereby suggesting a similar phenotypic response in all animals.

Conclusions

In a murine model of MF, moderate dynamic exercise prevented aortic root dilation and mitigates cardiac hypertrophy. Our data invite validation in other animal models of MF and eventually in patients.

Acknowledgments

Sources of Funding

Disclosures

None.

References

1. Dietz HC, Cutting GR, Pyeritz RE, Maslen CL, Sakai LY, Corson GM, Puffenberger EG, Hamosh A, Nanthakumar EJ, Curristin SM. Marfan syndrome caused by a recurrent de novo missense mutation in the fibrillin gene. *Nature*. 1991;352:337–339.

2. Doyle JJ, Gerber EE, Dietz HC. Matrix-dependent perturbation of TGFβ signaling and disease. *FEBS Lett*. 2012;586:2003–2015.

3. Perrucci GL, Rurali E, Gowran A, Pini A, Antona C, Chiesa R, Pompilio G, Nigro P. Vascular smooth muscle cells in Marfan syndrome aneurysm: the broken bricks in the aortic wall. *Cell Mol Life Sci*. 2017;74:267–277.

4. Singh MN, Lacro RV. Recent clinical drug trials evidence in Marfan syndrome and clinical implications. *Can J Cardiol*. 2015;32:66–77.

5. Hiratzka LF, Bakris GL, Beckman JA, Bersin RM, Carr VF, Casey DE, Eagle KA, Hermann LK, Isselbacher EM, Kazerooni EA, Kouchoukos NT, Lytle BW,

Milewicz DM, Reich DL, Sen S, Shinn JA, Svensson LG, Williams DM; American College of Cardiology Foundation/American Heart Association Task Force on Practice Guidelines, American Association for Thoracic Surgery, American College of Radiology, American Stroke Association, Society of Cardiovascular Anesthesiologists, Society for Cardiovascular Angiography and Interventions, Society of Interventional Radiology, Society of Thoracic Surgeons, Society for Vascular Medicine. 2010 ACCF/AHA/AATS/ACR/ASA/SCA/SCAI/SIR/STS/SVM guidelines for the diagnosis and management of patients with Thoracic Aortic Disease: a report of the American College of Cardiology Foundation/American Heart Association Task Force on Practice Guidelines, American Association for Thoracic Surgery, American College of Radiology, American Stroke Association, Society of Cardiovascular Anesthesiologists, Society for Cardiovascular Angiography and Interventions, Society of Interventional Radiology, Society of Thoracic Surgeons, and Society for Vascular Medicine. *Circulation*. 2010;121:e266–e369.

6. Campens L, Renard M, Trachet B, Segers P, Muino Mosquera L, De Sutter J, Sakai L, De Paepe A, De Backer J. Intrinsic cardiomyopathy in Marfan syndrome: results from in-vivo and ex-vivo studies of the Fbn1C1039G/+ model and longitudinal findings in humans. *Pediatr Res*. 2015;78:256–263.

7. Cook JR, Carta L, Bénard L, Chemaly ER, Chiu E, Rao SK, Hampton TG, Yurchenco P; GenTAC Registry Consortium, Costa KD, Hajjar RJ, Ramirez F. Abnormal muscle mechanosignaling triggers cardiomyopathy in mice with Marfan syndrome. *J Clin Invest*. 2014;124:1329–1339.

8. Cohn RD, van Erp C, Habashi JP, Soleimani AA, Klein EC, Lisi MT, Gamradt M, ap Rhys CM, Holm TM, Loeys BL, Ramirez F, Judge DP, Ward CW, Dietz HC. Angiotensin II type 1 receptor blockade attenuates TGF-beta-induced failure of muscle regeneration in multiple myopathic states. *Nat Med*. 2007;13:204–210.

9. Schuler G, Adams V, Goto Y. Role of exercise in the prevention of cardiovascular disease: results, mechanisms, and new perspectives. *Eur Heart J*. 2013;34:1790–1799.

10. Volianitis S, Secher NH. Cardiovascular control during whole body exercise. *J Appl Physiol*. 2016;121:376–390.

11. Iskandar A, Thompson PD. A meta-analysis of aortic root size in elite athletes. *Circulation*. 2013;127:791–798.

12. Braverman AC, Harris KM, Kovacs RJ, Maron BJ. Eligibility and disqualification recommendations for competitive athletes with cardiovascular abnormalities: Task Force 7: aortic diseases, including Marfan syndrome: a scientific statement from the American Heart Association and American College of Cardiology. *J Am Coll Cardiol*. 2015;66:2398–2405.

13. Cheng A, Owens D. Marfan syndrome, inherited aortopathies and exercise: what is the right answer? *Heart*. 2015;101:752–757.

14. Judge DP, Biery NJ, Keene DR, Geubtner J, Myers L, Huso DL, Sakai LY, Dietz HC. Evidence for a critical contribution of haploinsufficiency in the complex pathogenesis of Marfan syndrome. *J Clin Invest*. 2004;114:172–181.

15. Hirata K, Triposkiadis F, Sparks E, Bowen J, Wooley CF, Boudoulas H. The Marfan syndrome: abnormal aortic elastic properties. *J Am Coll Cardiol*. 1991;18:57–63.

16. Claus P, Weidemann F, Dommke C, Bito V, Heinzel FR, D'hooge J, Sipido KR, Sutherland GR, Bijnens B. Mechanisms of postsystolic thickening in ischemic myocardium: mathematical modelling and comparison with experimental ischemic substrates. *Ultrasound Med Biol*. 2007;33:1963–1970.

17. Kim EK, Choi SH, Sung K, Kim WS, Choe YH, Oh JK, Kim D-K. Aortic diameter predicts acute type A aortic dissection in patients with Marfan syndrome but not in patients without Marfan syndrome. *J Thorac Cardiovasc Surg*. 2014;147:1505–1510.

18. Jondeau G, Boutouyrie P, Lacolley P, Laloux B, Dubourg O, Bourdarias JP, Laurent S. Central pulse pressure is a major determinant of ascending aorta dilation in Marfan syndrome. *Circulation*. 1999;99:2677–2681.

19. Kohler M, Blair E, Risby P, Nickol AH, Wordsworth P, Forfar C, Stradling JR. The prevalence of obstructive sleep apnoea and its association with aortic dilatation in Marfan's syndrome. *Thorax*. 2009;64:162–166.

20. Benke K, Agg B, Matyas G, Szokolai V, Harsanyi G, Szilveszter B, Odler B, Polos M, Maurovich-Horvat P, Radovits T, Merkely B, Nagy ZB, Szabolcs Z. Gene polymorphisms as risk factors for predicting the cardiovascular manifestations in Marfan syndrome. Role of folic acid metabolism enzyme gene polymorphisms in Marfan syndrome. *Thromb Haemost*. 2015;114:748–756.

21. Akazawa Y, Motoki N, Tada A, Yamazaki S, Hachiya A, Matsuzaki S, Kamiya M, Nakamura T, Kosho T, Inaba Y. Decreased aortic elasticity in children with Marfan syndrome or Loeys-Dietz syndrome. *Circ J*. 2016;80:2369–2375.

22. Groenink M, de Roos A, Mulder BJ, Verbeeten B, Timmermans J, Zwinderman AH, Spaan JA, van der Wall EE. Biophysical properties of the normal-sized aorta in patients with Marfan syndrome: evaluation with MR flow mapping. *Radiology*. 2001;219:535–540.

23. Chung AWY, Au Yeung K, Sandor GGS, Judge DP, Dietz HC, Van Breemen C. Loss of elastic fiber integrity and reduction of vascular smooth muscle contraction resulting from the upregulated activities of matrix metalloproteinase-2 and -9 in the thoracic aortic aneurysm in Marfan syndrome. *Circ Res*. 2007;101:512–522.

24. Sabatier L, Chen D, Fagotto-Kaufmann C, Hubmacher D, McKee MD, Annis DS, Mosher DF, Reinhardt DP. Fibrillin assembly requires fibronectin. *Mol Biol Cell*. 2009;20:846–858.

25. Syyong HT, Chung AWY, Yang HHC, Van Breemen C. Dysfunction of endothelial and smooth muscle cells in small arteries of a mouse model of Marfan syndrome. *Br J Pharmacol*. 2009;158:1597–1608.

26. Bunton TE, Biery NJ, Myers L, Gayraud B, Ramirez F, Dietz HC. Phenotypic alteration of vascular smooth muscle cells precedes elastolysis in a mouse model of Marfan syndrome. *Circ Res*. 2001;88:37–43.

27. Oller J, Méndez-Barbero N, Ruiz EJ, Villahoz S, Renard M, Canelas LI, Briones AM, Alberca R, Lozano-Vidal N, Hurlé MA, Milewicz D, Evangelista A, Salaices M, Nistal JF, Jiménez-Borreguero LJ, De Backer J, Campanero MR, Redondo JM. Nitric oxide mediates aortic disease in mice deficient in the metalloprotease Adamts1 and in a mouse model of Marfan syndrome. *Nat Med*. 2017;23:200–212.

28. Silva JF, Correa IC, Diniz TF, Lima PM, Santos RL, Cortes SF, Coimbra CC, Lemos VS. Obesity, inflammation, and exercise training: relative contribution of iNOS and eNOS in the modulation of vascular function in the mouse aorta. *Front Physiol*. 2016;7:1–13.

29. Kleindienst A, Battault S, Belaidi E, Tanguy S, Rosselin M, Boulghobra D, Meyer G, Gayrard S, Walther G, Geny B, Durand G, Cazorla O, Reboul C. Exercise does not activate the β3 adrenergic receptor–eNOS pathway, but reduces inducible NOS expression to protect the heart of obese diabetic mice. *Basic Res Cardiol*. 2016;111:40.

30. Tae H-J, Petrashevskaya N, Marshall S, Krawczyk M, Talan M. Cardiac remodeling in the mouse model of Marfan syndrome develops into two distinctive phenotypes. *Am J Physiol Heart Circ Physiol*. 2016;310:H290–H299.

31. Kiotsekoglou A, Saha S, Moggridge JC, Kapetanakis V, Govindan M, Alpendurada F, Mullen MJ, Nassiri DK, Camm J, Sutherland GR, Bijnens BH, Child A. Impaired biventricular deformation in Marfan syndrome: a strain and strain rate study in adult unoperated patients. *Echocardiography*. 2011;28:416–430.

32. De Backer JF, Devos D, Segers P, Matthys D, François K, Gillebert TC, De Paepe AM, De Sutter J. Primary impairment of left ventricular function in Marfan syndrome. *Int J Cardiol*. 2006;112:353–358.

33. Savolainen A, Kupari M, Toivonen L, Kaitila I, Viitasalo M. Abnormal ambulatory electrocardiographic findings in patients with the Marfan syndrome. *J Intern Med*. 1997;241:221–226.

34. Kokkinos PF, Narayan P, Colleran JA, Pittaras A, Notargiacomo A, Reda D, Papademetriou V. Effects of regular exercise on blood pressure and left ventricular hypertrophy in African-American men with severe hypertension. *N Engl J Med*. 1995;333:1462–1467.

35. Konhilas JP, Watson PA, Maass A, Boucek DM, Horn T, Stauffer BL, Luckey SW, Rosenberg P, Leinwand LA. Exercise can prevent and reverse the severity of hypertrophic cardiomyopathy. *Circ Res*. 2006;98:540–548.

36. Medeiros WM, Peres PA, Carvalho AC, Gun C, De Luca FA. Effect of a physical exercise program in a patient with Marfan syndrome and ventricular dysfunction. *Arq Bras Cardiol*. 2012;98:e70–e73.

37. Guasch E, Mont L. Diagnosis, pathophysiology, and management of exercise-induced arrhythmias. *Nat Rev Cardiol*. 2017;14:88–101.

38. Calvo N, Ramos P, Montserrat S, Guasch E, Coll-Vinent B, Domenech M, Bisbal F, Hevia S, Vidorreta S, Borras R, Falces C, Embid C, Montserrat JM, Berruezo A, Coca A, Sitges M, Brugada J, Mont L. Emerging risk factors and the dose-response relationship between physical activity and lone atrial fibrillation: a prospective case-control study. *Europace*. 2016;18:57–63.

39. James CA, Bhonsale A, Tichnell C, Murray B, Russell SD, Tandri H, Tedford RJ, Judge DP, Calkins H. Exercise increases age-related penetrance and arrhythmic risk in arrhythmogenic right ventricular dysplasia/cardiomyopathy-associated desmosomal mutation carriers. *J Am Coll Cardiol*. 2013;62:1290–1297.

40. Sawant AC, Te Riele ASJM, Tichnell C, Murray B, Bhonsale A, Tandri H, Judge DP, Calkins H, James CA. Safety of American Heart Association-recommended minimum exercise for desmosomal mutation carriers. *Heart Rhythm*. 2016;13:199–207.

41. Wisløff U, Helgerud J, Kemi OJ, Ellingsen O. Intensity-controlled treadmill running in rats: VO(2 max) and cardiac hypertrophy. *Am J Physiol Heart Circ Physiol*. 2001;280:H1301–H1310.

SUPPLEMENTAL MATERIAL

**Figure S1.** Intramyocardial artery assessment.
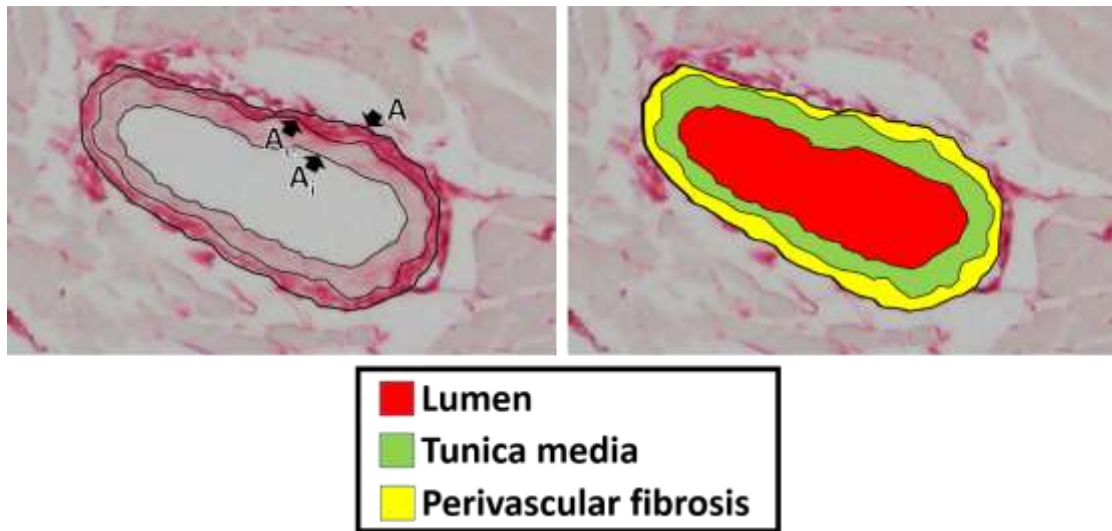
First, the perivascular area (**A**, limited by perivascular fibrosis), the external area (**Ae**, limited by outer tunica adventitia) and internal area (**Ai**, limited by internal elastic lamina) were identified and limits traced (left pannel). Thereafter, the area within each of these limits was automatically quantified. Perivascular fibrosis was then calculated as A – Ae (yellow area in the right panel); tunica media area was calculated as Ae – Ai (green area in the right panel); and luminal area was identified as Ai (red area in the right panel).

Figure S2. Survival rate during the experimental protocol in all groups.
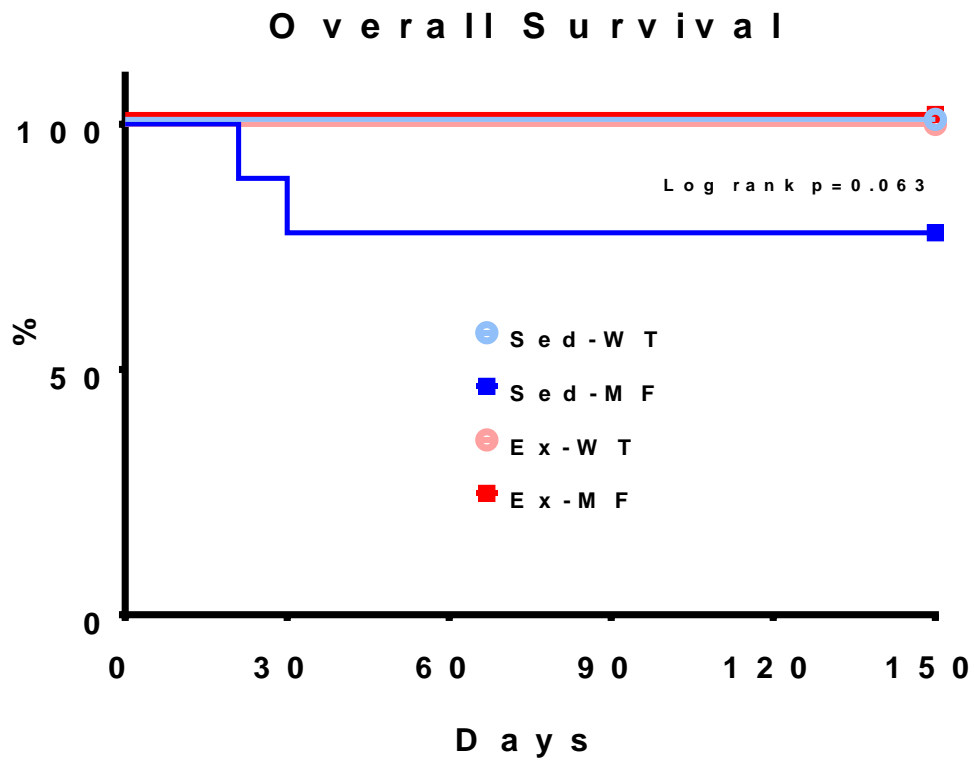

Analysis with Log-rank test. WT: wild-type; MF: Marfan; Sed: sedentary group; Ex: trained group.

**Figure S3.** *Vastus medialis* adaptation after training.
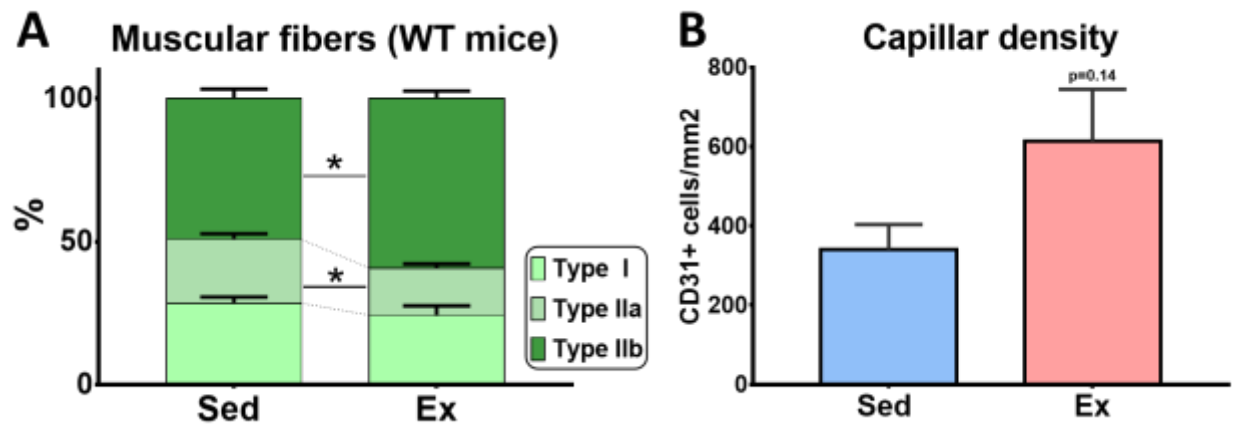
 (A) Proportion of muscular fibers according to its oxidative status (n=9 per group). (B) Capilar density evaluated in CD31 immunohistochemistry stained samples (n=6 per group). *p<0.05 Sed vs Ex. WT: wild-type; Sed: sedentary group; Ex: trained group.

Figure S4. Blood pressure measurement in all groups according to sex (for male animals: n=5 for all WT-Sed, MF-Sed, MF-Sed and MF-Ex; for female animals: n= 6 for WT-Sed; n=4 for MF-Sed; n=5 for WT-Ex; n=5 for MF-Ex).
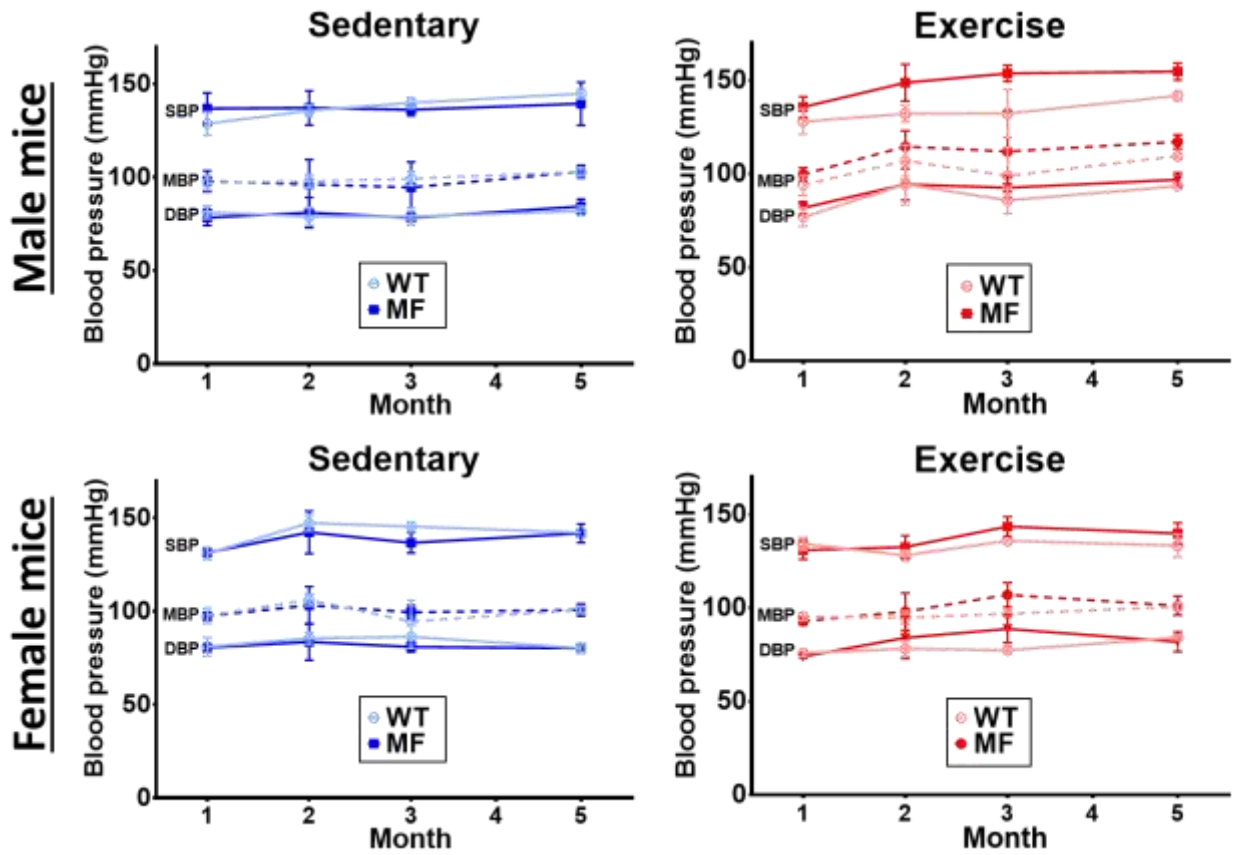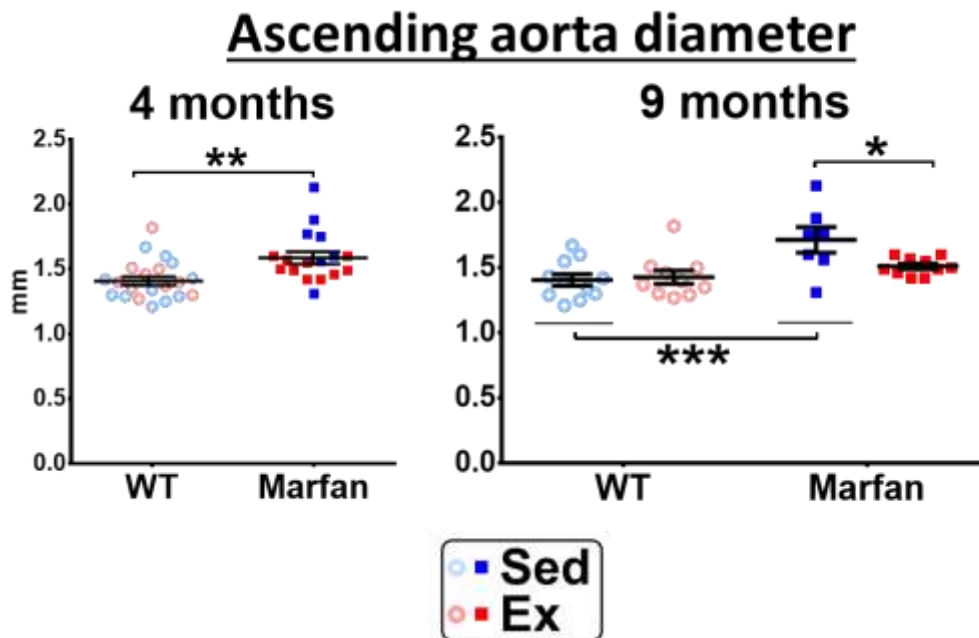

WT: wild-type; MF: Marfan.

Figure S5. Changes of the aortic root size during the experimental protocol examined for each mouse (at 4 months and at 9 months; n=11 for WT-Sed, n=10 for WT-Ex, n=7 for MF-Sed, n=10 for MF-Ex).
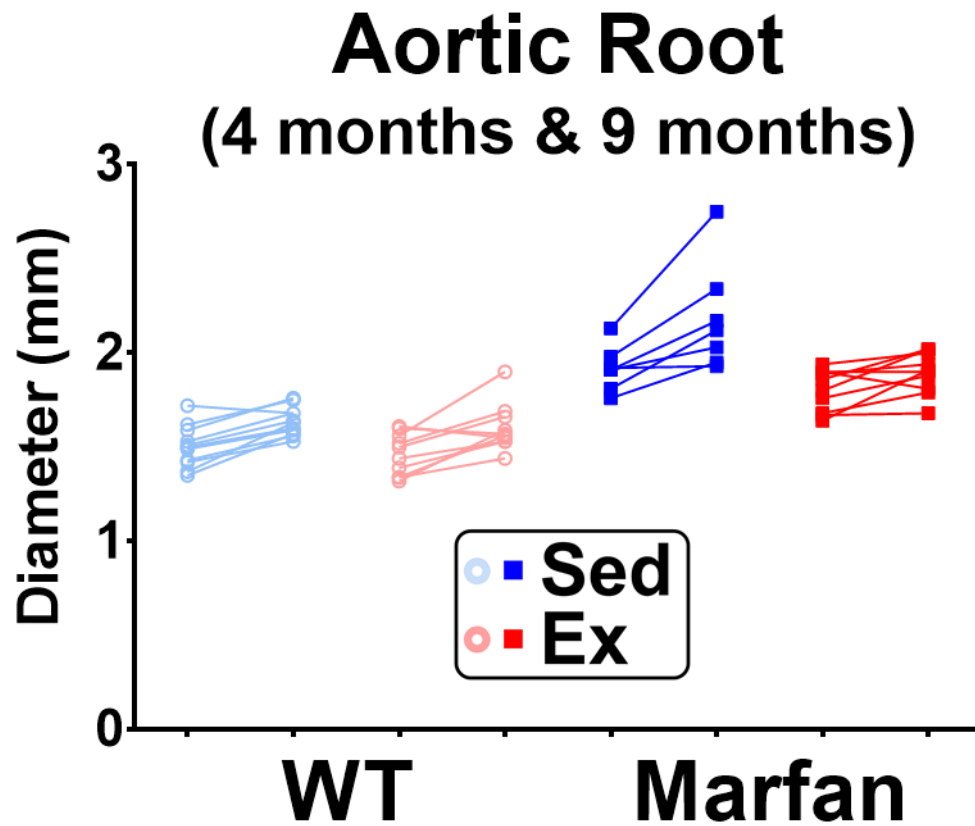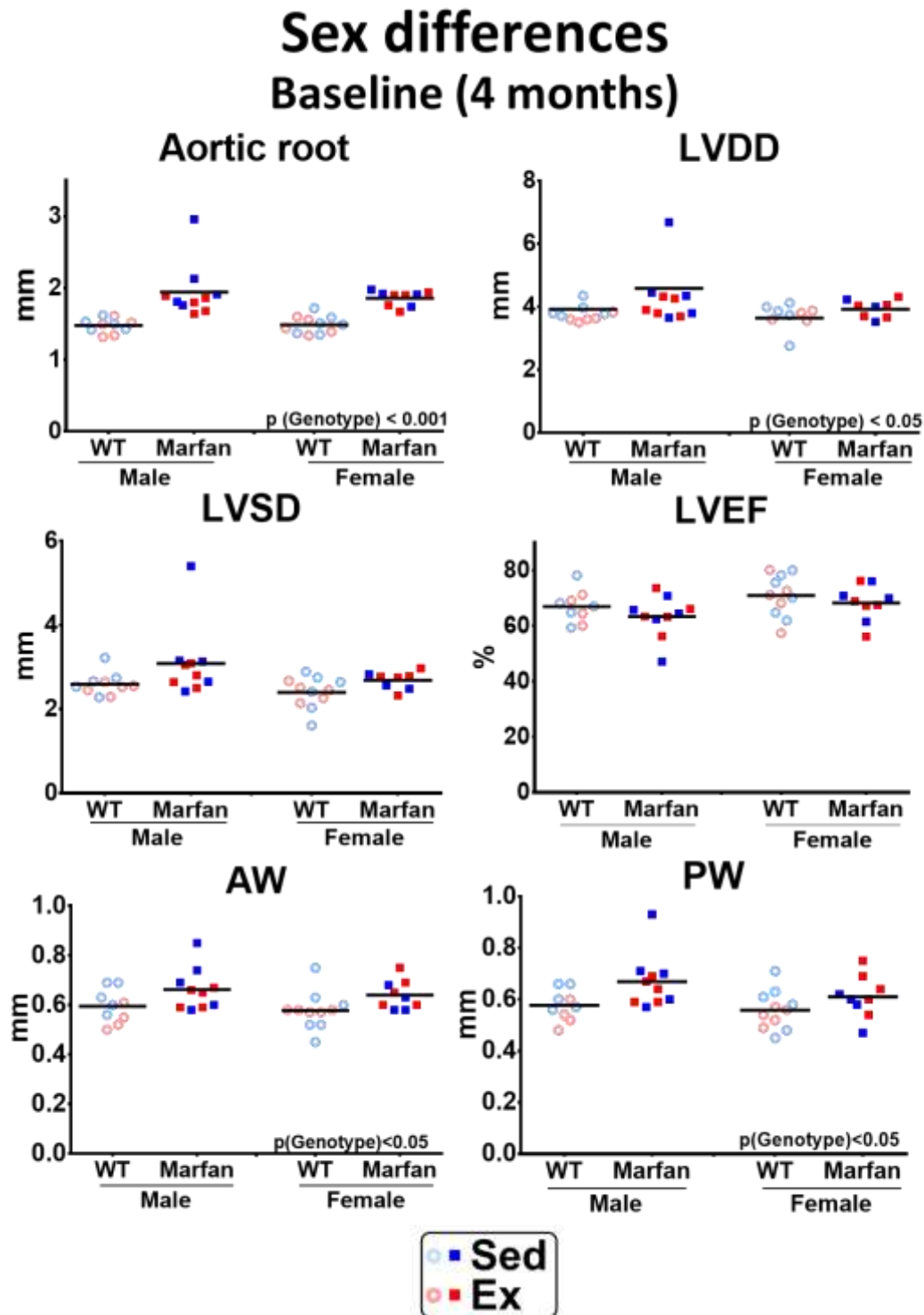

Open circles represent WT mice, closed squares represent Marfan mice; blue symbols are sedentary mice, red symbols are trained mice. WT: wild-type; MF: Marfan; Sed: sedentary group; Ex: trained group.

Figure S6. Measurements of the ascending aorta in all groups at the 4-month time-point (left panel; comparison with a *t*-test; n=21 for WT, n=17 for MF) and at the 9-month time-point (right panel; comparison with two-way ANOVA; significant interaction was found; n=11 for WT-Sed, n=7 for MF-Sed, n=10 for WT-Ex, n=10 for MF-Ex).

*p<0.05; **p<0.01; ***p<0.001. WT: wild-type; MF: Marfan; Sed: sedentary group; Ex: trained group. Open circles represent WT mice, closed squares represent Marfan mice; blue symbols are sedentary mice, red symbols are trained mice.

Figure S7. Echocardiographic results according to sex at the 4-month time point (for most measurements: male mice n=10 for both WT and MF; female mice; n=11 for WT, n=9 for MF).

Comparisons were carried out with 2-way ANOVA (genotype [WT, MF], sex and genotype x sex). No significant interaction was found in any comparison. WT: wild-

type; MF: Marfan; Sed: sedentary group; Ex: trained group; LVEDD: left ventricle end-diastolic diameter; LVESD: left ventricle end-systolic diameter; AW: anterior wall; PW: posterior wall; LVEF: left ventricular ejection fraction. Open circles represent WT mice, closed squares represent Marfan mice; blue symbols are sedentary mice, red symbols are trained mice.

Figure S8. Echocardiographic results according to sex at the 9-month time point (n=3-6 per group).
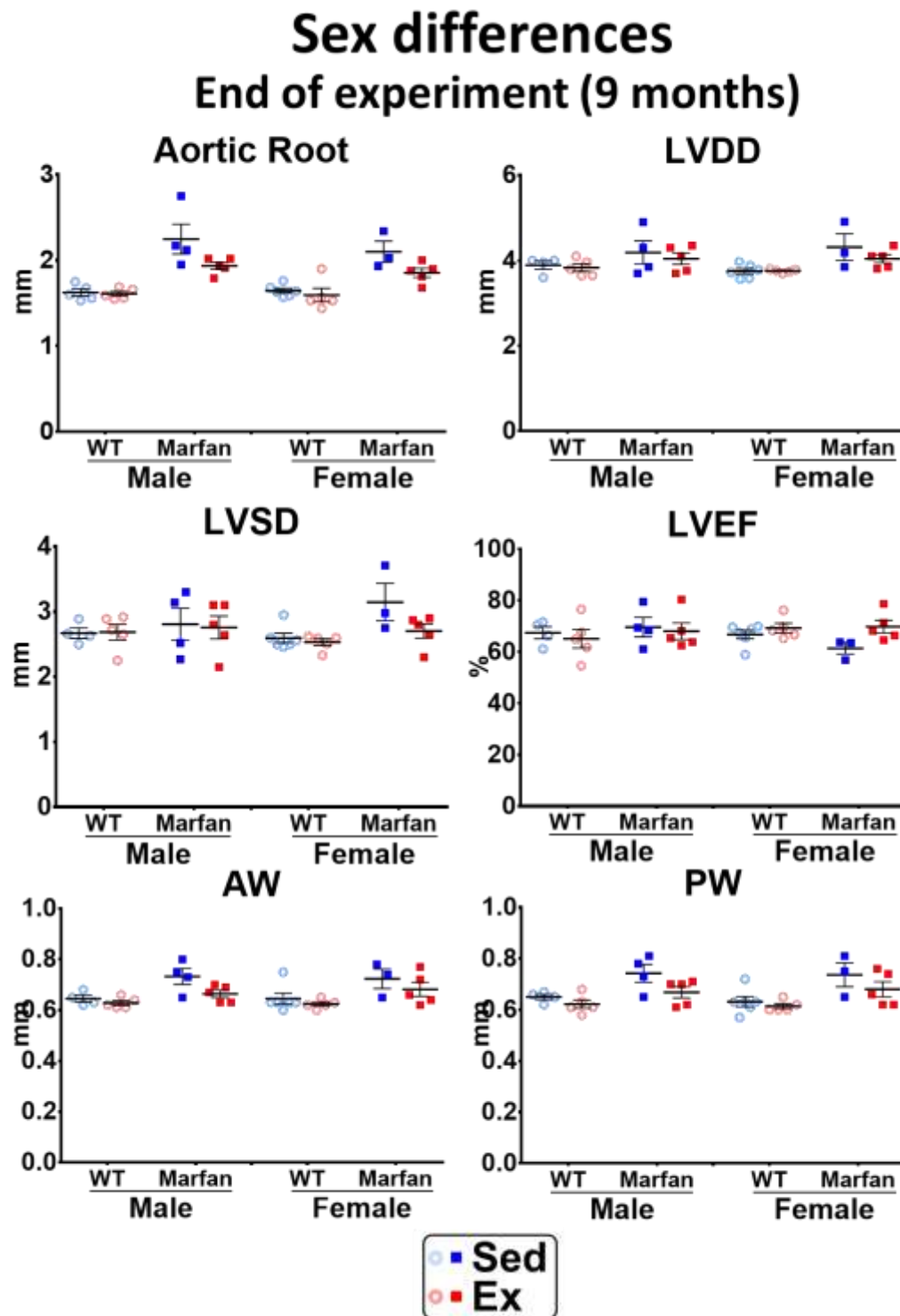
Comparisons were carried out with 2-way ANOVA (genotype [WT, MF], sex and genotype x sex). No significant interaction was found in any comparison. WT: wild-type; MF: Marfan; Sed: sedentary group; Ex: trained group; LVEDD: left ventricle end-

diastolic diameter; LVESD: left ventricle end-systolic diameter; AW: anterior wall; PW: posterior wall; LVEF: left ventricular ejection fraction. Open circles represent WT mice, closed squares represent Marfan mice; blue symbols are sedentary mice, red symbols are trained mice.

Figure S9. Effects of sex on LV histological assessment (n=3-6 per group).
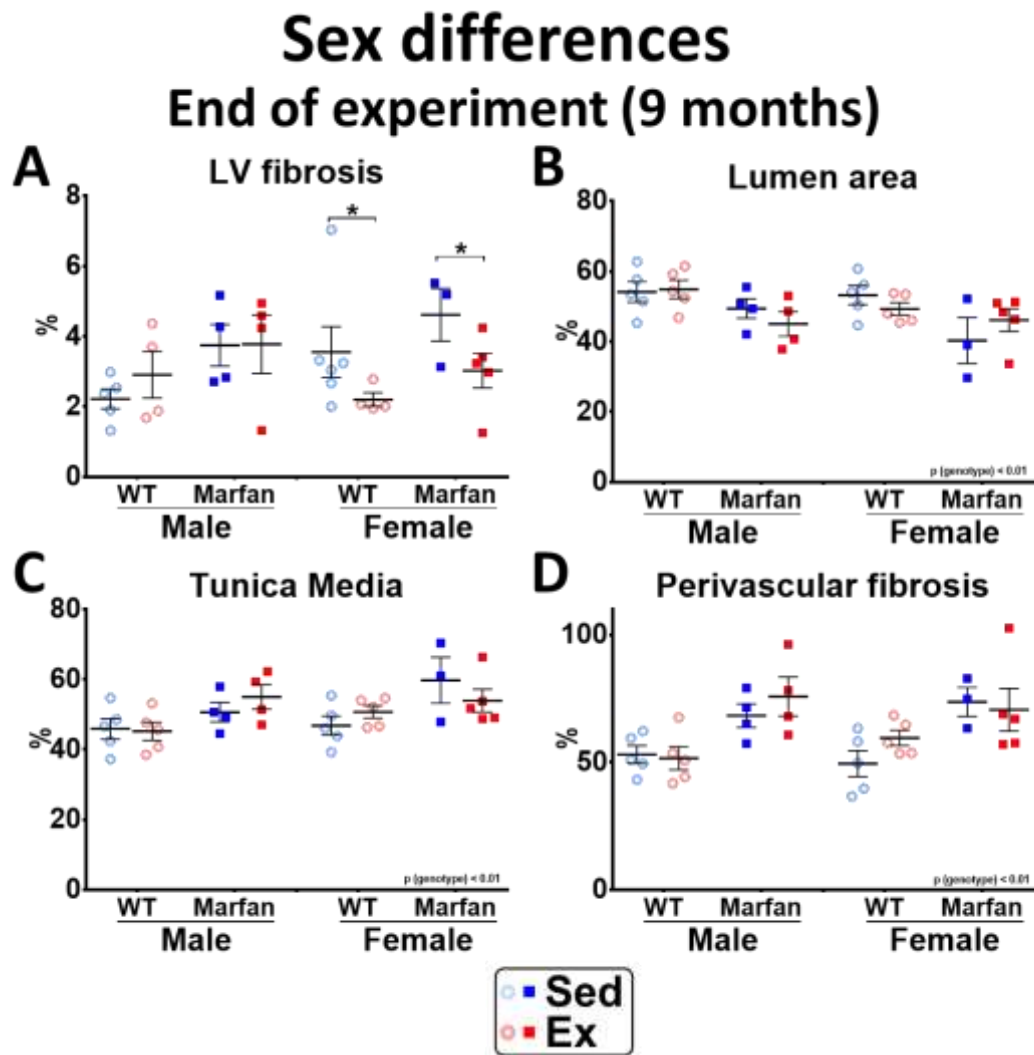
(A) LV fibrosis; (B) Lumen area of intramyocardial arteries; (C) Tunica media of intramyocardial arteries; (D) Perivascular fibrosis of intramyocardial arteries. Analyses performed with a three-way ANOVA. For panel A, a Sex x Group interaction was found (p=0.02); pairwise comparisons (Sed vs Ex within each Sex) are shown. In panels B, C and D, no significant effect of sex or their interactions was found. *P<0.05. WT: wild-type; MF: Marfan; Sed: sedentary group; Ex: trained group; LVEDD: left ventricle end-diastolic diameter; LVESD: left ventricle end-systolic diameter; AW: anterior wall; PW: posterior wall; LVEF: left ventricular ejection fraction. Open circles represent WT mice, closed squares represent Marfan mice; blue symbols are sedentary mice, red symbols are trained mice.